Journal of Mechanical Engineering Research and Developments
ISSN: 1024-1752
CODEN: JERDFO
Vol. 44, No. 4, pp. 233-242
Published Year 2021

Effect of Addition Ag and Cu Nanoparticles on Electrochemical Discharge Machining of NiTi Shape Memory Alloys

Shahad Ali Hammood[†], Haydar Al-Ethari[†], Abdolreza Rahimi[‡]

[†] Department of Metallurgical Engineering, College of Material's Eng., University of Babylon, Hilla, Iraq.
[‡] Dept. of Mechanical Eng., College of Engineering, University of Amirkabir-Tahran-Iran.

*Corresponding Author Email: shahad.alkawaz@uobabylon.edu.iq, dralethariah@yahoo.com, rahimi@aut.ac.ir

ABSTRACT

Nitinol as a shape memory alloy is widely used in engineering applications. Most of such applications required machining processes, which may particularly influence the product as a specified functional material. In this experimental study, holes of 1 mm diameter were drilled to the nitinol alloy and nitinol with addition of 0.5wt% nanoparticles of each copper and silver. Electrochemical discharge machining was used where surface characteristics of the machined alloys, metal removal rate, and tool wear rate were investigated. The experimental results indicate that the alloy with silver and copper has a better metal removal rate (0.0885 mg/sec) at voltage 80V and solution concentration 40%, lower surface roughness (0.00996 µm) at voltage 50V and solution concentration 30%, lower white layer thickness (2.5167 µm) at voltage 50V and solution concentration 40%, and lower surface crack density (0.0047 µm/µm^2) at voltage 50V and solution concentration 40%, but a higher tool wear rate than the base alloy.

KEYWORDS

Electrochemical Discharge Machining, Nanoparticles, Material Removal Rate, Tool Wear Rate, Surface Roughness, White Layer Thickness, Surface Crack Density.

INTRODUCTION

The Shape memory alloys (SMAs) are a class of metallic alloys that are capable of suffering from large displacements while returning to their original undeformed shape via either the application of heat due to shape memory effect or elimination of the load, due to superelastic effect. Nickel-titanium alloys are the most common type of these alloys due to their ability to regain their original shape after distortion [1]. The addition of silver and copper to the nickel–titanium alloy rises the corrosion resistance and excellent antibacterial characteristics. Silver stabilizes the martensitic phase at room temperature, while copper rises the characteristics *temperatures* of the martensitic transformation. For biomedical applications in orthodontic, human bone, and other applications, NiTiAg and NiTiCu alloys are suitable [2, 3].

Nickel-titanium alloys are difficult to machine by the traditional method. Unconventional strain hardening behavior, high ductility, low thermal conductivity, and high tool wear are responsible for the poor machinability of NiTi alloy. Therefore non-conventional methods are utilized to overcome some of these problems. Electrodischarge machining (EDM), laser machining (LBM), abrasive water jet machining (AWJM), and many other methods are applied to machine NiTi parts [4]. Many attempts were conducted to obtain the machined parts with lower influence on their functional characteristics. Pfeifer R. et. al [5] studied the influence of process parameters of laser machining of NiTi SMA. Kong MC. et al [6] investigated geometrical accuracy and surface integrity in abrasive water jet machining of NiTi SMA. Mareike Frensemeier, et.al. [7] utilized pulse electrochemical machining (PECM) to machine the NiTi alloy. Ali Alidoosti et. al. [8] used two different electrode materials (copper electrode and tungsten-copper (W-Cu) electrode) to investigate the electrical discharge machining characteristics of NiTi shape memory alloys.

Alana Witt Hansena et. al. [9] evaluated the electrochemical behavior of polished NiTi surfaces exposed to various simulated body fluid solutions: Hanks solution, Hanks' balanced salt (HBSS) solution, saline body

fluids (SBF) solution, and Ringer solution. Al-Ethari et. al. [10] investigated on Chemical Machining of NiTi SMA prepared by powder metallurgy route. Robert Roth et. al. [11] used electrical discharge machining (EDM) of biocompatible Nitinol that combines superelasticity, great precision of fabrication, and miniaturization capabilities, thus presenting a promising base material for flexible medical instruments in minimally invasive surgery. This research work presents an investigation on the influence of electrochemical discharge machining (ECDM) on the surface roughness, the thickness of the white layer, the surface crack density of machined specimen fabricated from NiTi using powder metallurgy route. The investigation includes, also, the metal removal rate and the tool wear rate. Nanoparticles of Cu & Ag were added to the NiTi base alloy to investigate the improvement of its machining characteristics through the use of process parameters (voltage, and solution concentration).

EXPERIMENTAL DETAILS

Materials and Processing

The powder metallurgy method was utilized to prepare the Nickel-Titanium shape memory alloys. Two alloy samples were fabricated. The particle size of the powders used to fabricate the samples and the codes for these samples are demonstrated in table (1). A compacting pressure of 650 MPa was utilized to make cylindrical compacts of 13 mm diameter and 5 mm height via uniaxial and double action steel die on a hydraulic press type (CT340-CT440). The sintering of the compacts was performed in tube furnace type ((model GSL 1600X, China) with an argon atmosphere. The green compacts were heated in the furnace to 550˚C, soaked for 1 hr, sintered at 850˚C for 5 hrs, then left in the furnace to cool to room temperature. The porosity of the sintered samples was measured according to ASTM B-328 [12], while the Vickers hardness was conducted at a loading of 500 g held for 10 seconds.

For the estimation of the average hardness, the specimen was indented five times at different locations. The shape memory effect (SME) was estimated based on the Brinell hardness test at room temperature. An indentation ball of 2.5mm diameter was used to measure the hardness of the sintered samples by applying a load of 187.5 kPs 10sec. An average of three readings has been recorded in this test. Subsequently the sample was heated to 800c for one hour in a vacuum furnace and left to cool inside the furnace. SME was determined according to the percentage of the difference between the average impression diameter in (μm) before and after heating to that before heating. The results of the hardness, porosity, and shape memory effect tests are demonstrated in table (1).

Table 1. Codes and the Properties of the Prepared Alloy Samples

Code of the alloy sample	**The constituents wt% and the particle size of the used powders**				**Hardness (HV)**	**Porosity (%)**	**Shape memory effect (%)**
	Ni 44.93μm	**Ti 99.17 μm**	**Cu 30 nm**	**Ag 80 nm**			
A_1	55	45	---	---	175	27	3
A_2	54	45	0.5	0.5	287	23	5

Machining Tests

Drilling of 1mm diameter holes was conducted utilizing (ZGA60FM-G7.8iN:1406A024, Japan) type at the University of Amirkabir/ college of mechanical engineering/Iran. Electrochemical discharge machine shown in figure1.

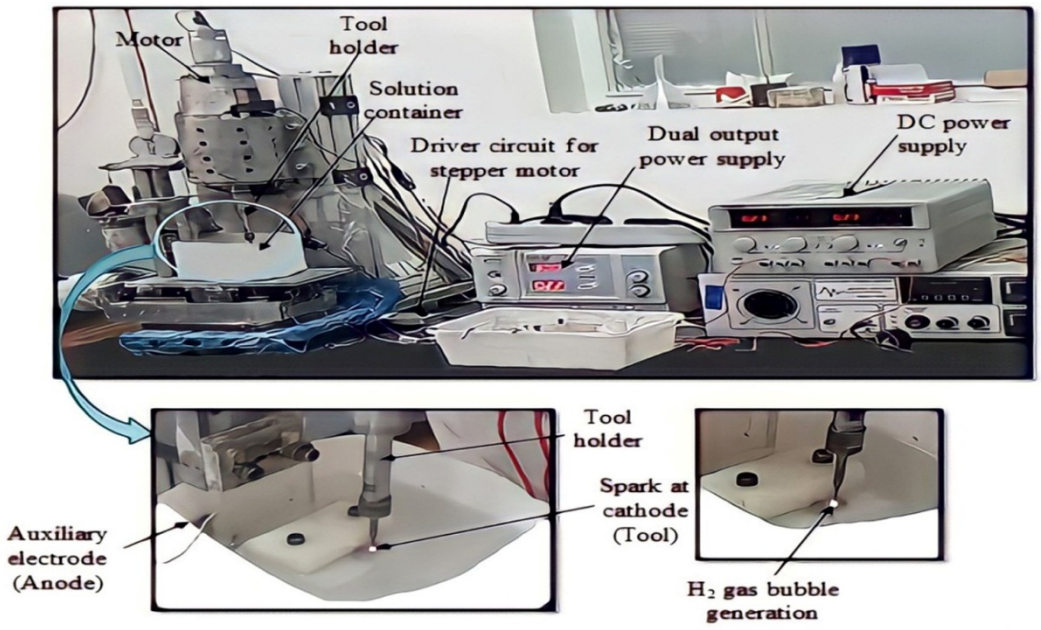

Figure 1. Electrochemical Discharge Machining Type (ZGA60FM-G7. 8iN:1406A024, Japan)

Specimens of 13mm diameter and 5mm height were used. Each face of the specimens was ground using 200 to 2000 size emery papers gradually and polished by 1µm diamond suspension before drilling. Tungsten carbide tool was utilized and settled in a steel tool holder type (C10-ER8-100L). In all tests, the gap between the tool electrode (cathode) and the workpiece was defined as 0.2mm. In all machining tests, sodium hydroxide NaOH with two concentrations (30 and 40%) was selected as the dielectric solution. Four values for the voltage (50, 60, 70, and 80V) as the machining conditions were selected. The ECDM process proceeded for 20 minutes. Oxygen gas is generated at the anode due to the following electrochemical reaction [13].

$$2H_2O \rightarrow O_2\uparrow + 4H^+ + 4e^- \quad (1)$$

Due to the following reaction hydrogen gas is generated at the cathode.

$$2H^+ + 2e^- \rightarrow H_2\uparrow (2)Na^+ + e^- \rightarrow Na \quad (2)$$

$$2Na + 2H_2O \rightarrow 2NaOH + H_2\uparrow \quad (3)$$

$$2H_2O + 2e^- \rightarrow H_2\uparrow + 2OH^- \quad (4)$$

The gas film is instantly broken-down when the applied machining voltage reaches the critical value, and a cluster of electric sparks is formed. To extract the work-piece material, the thermal energy released from the electric spark discharge is used and a micro-pit is thermally etched on its surface. The metal removal rate, tool wear rate, surface roughness, white layer thickness, and surface crack density were selected as the performance factors. The laser profilometer device type (LPM-D1-IRAN) was used to measure surface roughness. Material removal rate and tool wear rate were measured by weighing the specimen and the tool before and after the machining process as shown in Equations (5 & 6)[14]. After using wire electrical discharge machining (WEDM) to create a cross-section of the machining area for each sample [15], the white layer thickness can be determined by dividing the image area with the image length as shown in Eq.(7).

$$\text{MRR (mg/sec.)} = (IW)_w - (FW)_w / t \quad (5)$$

$$\text{TWR (mg/sec.)} = (IW)_T - (FW)_T / t \quad (6)$$

$$\text{White Layer Thickness (WLT)} = \text{Image Area/Image Length} \quad (7)$$

$$\text{Surface Crack Density (SCD)} = \text{Total Crack Length/Image Area} \quad (8)$$

MRR = Material removal rate (mg/sec).

TWR = Tool wear rate (mg/sec).
$(IW)_w$ = Original weight of the workpiece before machining, mg.
$(FW)_w$= Final weight of the workpiece after machining, mg.
$(IW)_т$ = Original weight of the tool before machining, mg.
$(FW)_т$ = Final weight of the tool after machining, mg.
t = Machining time, sec.

RESULTS AND DISCUSSION

Material Removal Rate (MRR)

The results of the material removal rate for A_1 and A_2 alloys are shown in figure 2.

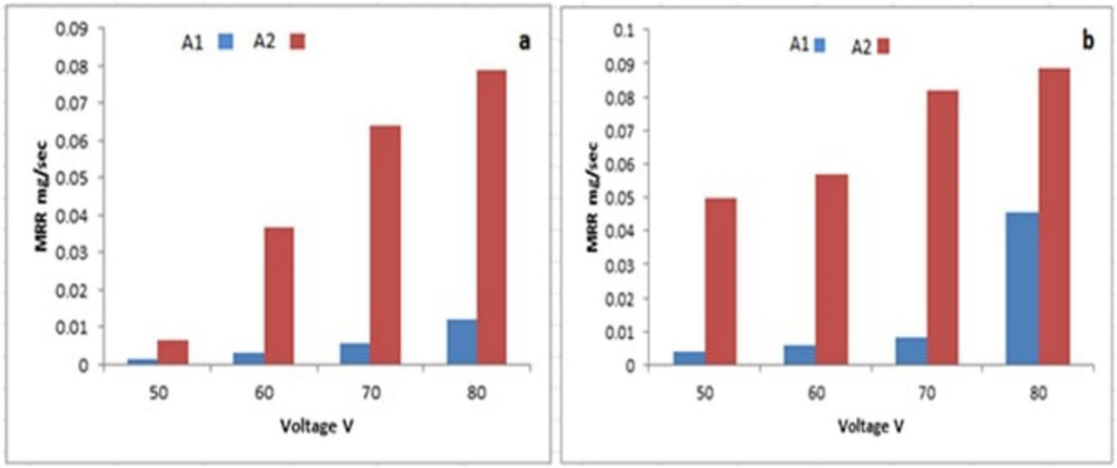

Figure 2. a) MRR results at solution concentration 30%, b) MRR results at solution concentration 40%

Figure 2 shows that MRR for A_2 alloy is higher than that for A_1 alloy at high voltage and high solution concentration. This is because when silver and copper are added, the thermal conductivity of the NiTi alloy increases, and then MRR increases. When the applied voltage increases, the amount of ions that hit the workpiece increases, which causes the intensity of the energy to increase. At higher electrolyte concentration, more electrochemical reactions occur between the tool and the auxiliary electrode, which in turn creates more gas bubbles at the sparking zone, with the generation of a larger number of sparks [16]. Figure 3 displays the scanning electron microscope image of hole shape that result from the ECDM process for A_1 and A_2 alloys with maximum material removal rate at voltage 80 V and solution concentration 40%.

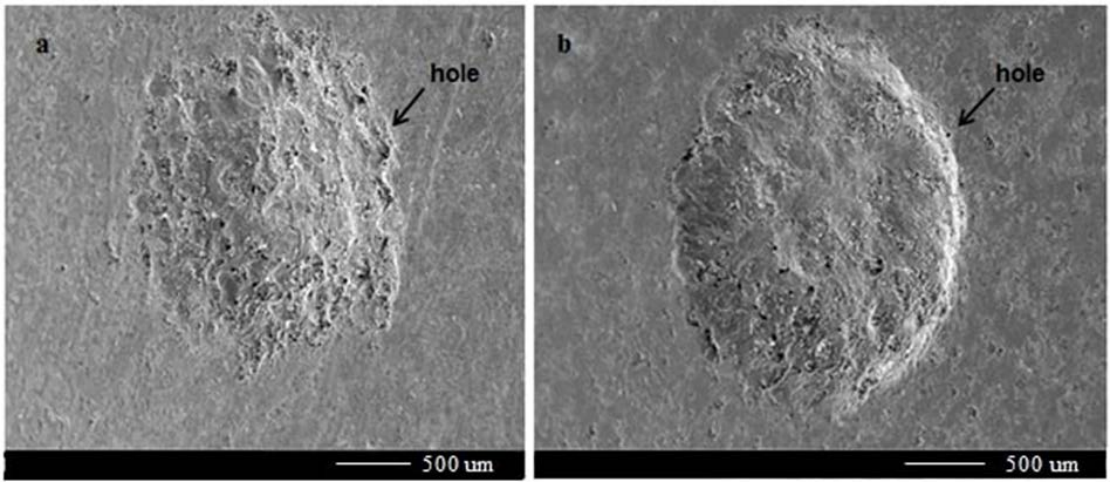

Figure 3. SEM Image of maximum Material removal rate from ECDM process at voltage 80 V and solution concentration 40% for a) A_1 alloy, b) A_2 alloy

It is clear from figure 3 that the material removal rate for A_2 alloy is higher than that for A_1 alloy and the hole shape for A_2 alloy is more regular.

Tool Wear Rate (TWR)

Figure 4 (a &b) displays the results of the tool wear rate of A_1 and A_2 alloys. Figure 5 (a & b) represents the scanning electron microscope image of tool wear for the tool which used in the ECDM process to machine A_1 and A_2 alloys.

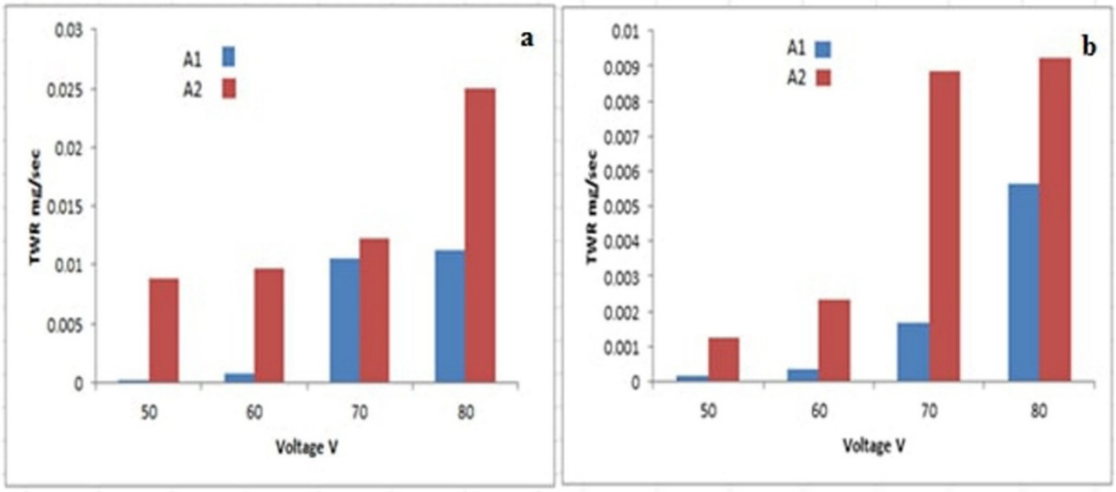

Figure 4. a) TWR results at solution concentration 30%, b) TWR results at solution concentration 40%.

Figure 4 (a & b) shows that A_2 alloy has high tool wear rate than A_1 alloy at high voltage and low solution concentration. With the rise of voltage, the energy of each pulse rises, and since one end of the pulse is on the tool and the other end is on the workpiece, this raises the amount of wear in the tool. The increase of voltage results in the rise of tool wear as most of the heat will be dissipated during tool materials than during workpiece or electrolyte [17]. TWR decreased with increased solution concentration. Figure 5 shows that A_2 alloy has a maximum tool wear rate than A_1 alloy because it has a higher hardness value than A_1 alloy.

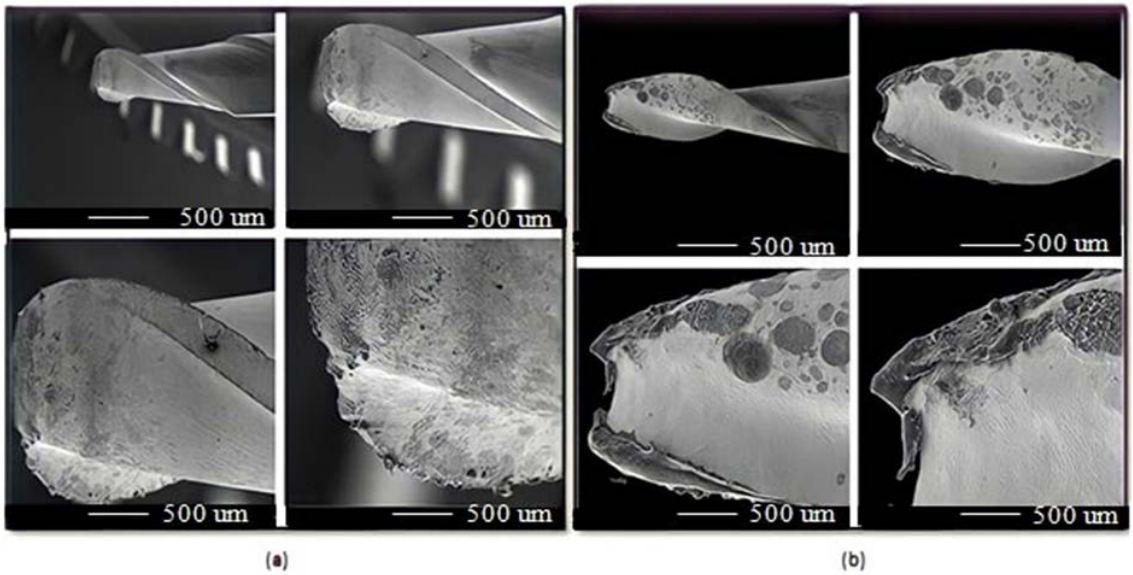

Figure 5. SEM Image of Maximum Tool Wear Rate at voltage 80 V and solution concentration 30% for a) A_1 alloy, b) A_2 alloy.

Surface Roughness (Ra).

Figure 6 shows the results of surface roughness of A_1 and A_2 alloys. Figure 7 displays a laser profilometer image of surface roughness for A_1 and A_2 alloys.

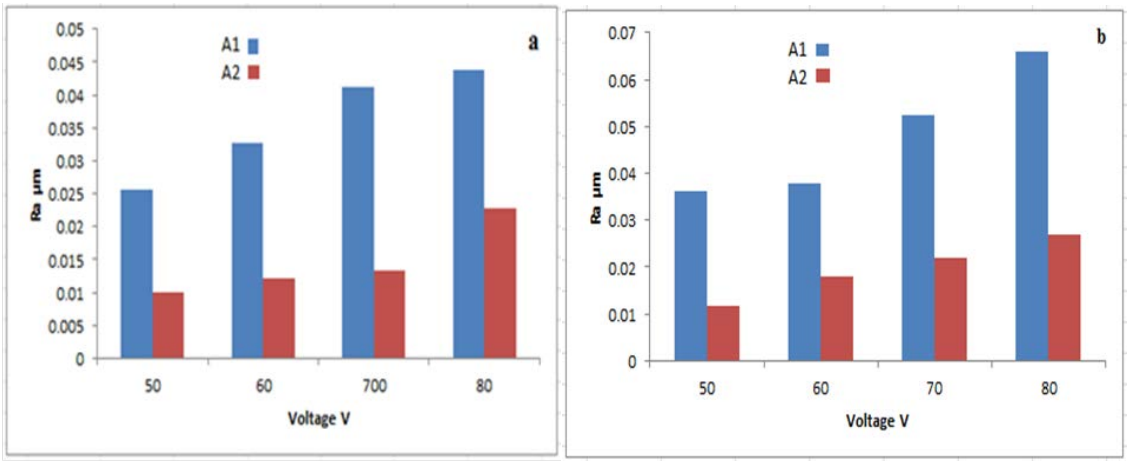

Figure 6. a) Surface Roughness Results at solution concentration 30%, b) Surface Roughness Results at Solution Concentration 40%

Figure 6 indicates that A_2 alloy has high surface quality rather than A_1 alloy with low surface roughness. As shown in figure 6, surface roughness, Ra, increased with the rise in voltage and solution concentration. The increase in voltage leads to an increase in spark energy, which causes the surface pits resulting from the material being removed to be enlarged.

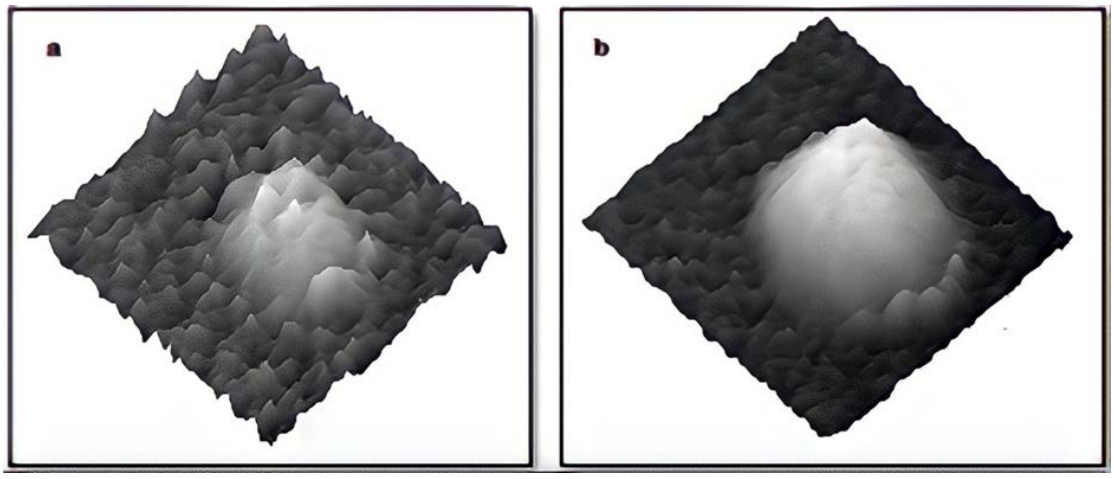

Figure 7. laser profilometer Image of high Surface Roughness at voltage 80 V and solution concentration 40% for a) A_1 alloy, b)A_2 alloy.

White Layer Thickness (WLT)

The white layer thickness outcomes for alloys at various voltage and solution concentration values are defined in Figure 8.

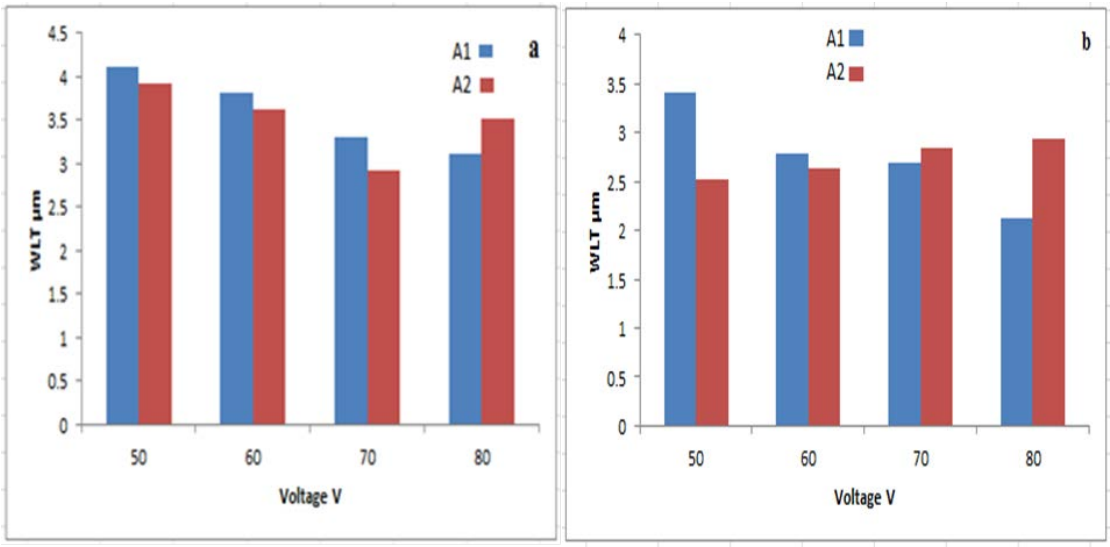

Figure 8. a) White Layer Thickness Results at solution concentration 30%, b) White Layer Thickness Results at solution concentration 40%.

As the voltage increases, the more heat is transmitted to the machined surface, the white layer thickness (WLT) is proportional to the voltage, leading to an increase in the quantity of molten metal. The quantity of molten metal that can be flushed away by a dielectric is considered constant, leading to the dielectric being increasingly unable to flush the molten material and thus building up as a white or recast layer on the machined surface [18]. The white layer thickness of the A_1 and A_2 alloys after machining is described in Figure (9) by scanning electron microscope image.

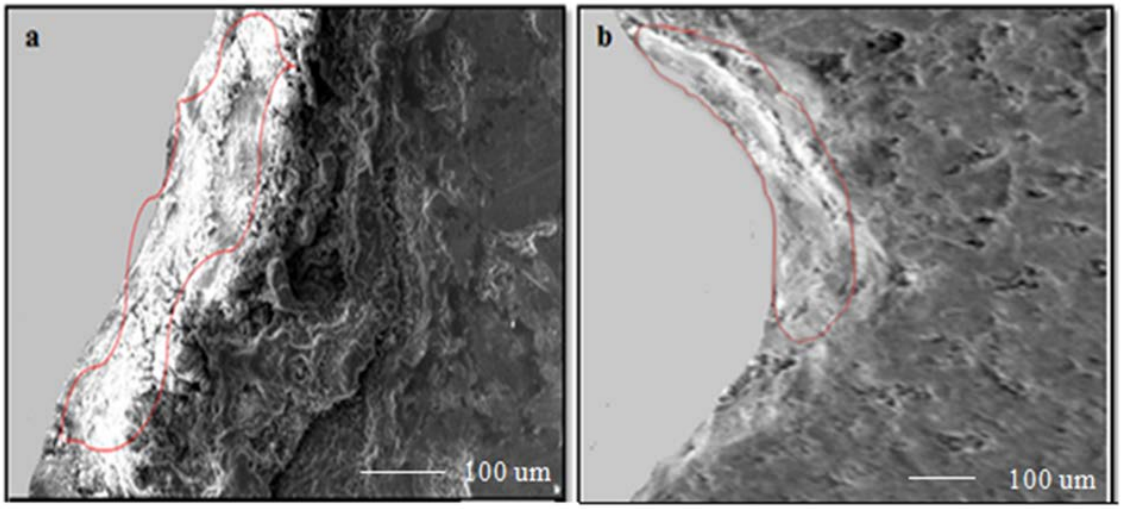

Figure 9. SEM Image of maximum white layer thickness at voltage 50 V and solution concentration 30% for a) A_1 alloy, b) A_2 alloy.

Figure 9 shows that the thickness of the white layer of the A_2 alloy was less than that of the A_1 alloy.

Surface Crack Density (SCD)

The surface crack density results for alloys are shown in Figure 10 (a & b). Figure (11) shows scanning electron microscope images of surface crack density for A_1 and A_2 alloys.

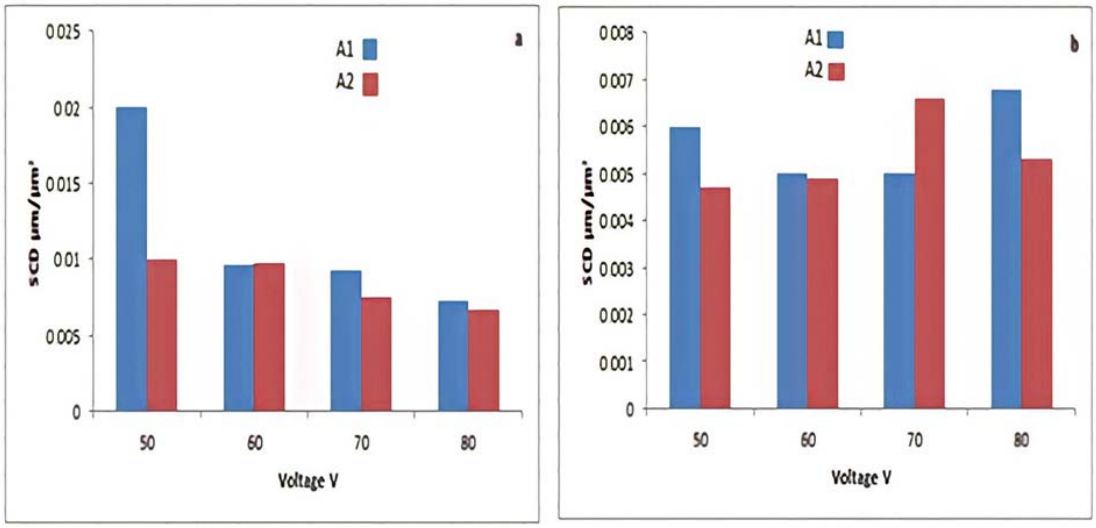

Figure 10. a) Surface Crack Density at Solution Concentration 30%, b) Surface Crack Density at Solution Concentration 40%.

The temperature produced during the machining process is greater than the melting point of the work-piece and is followed by rapid quenching. As a result, large thermal stresses are developed which exceed the fracture strength and thus, cracks are developed [19]. The A_2 alloy has a low surface crack density because this alloy has low porosity as shown in figure 10 and figure 11.

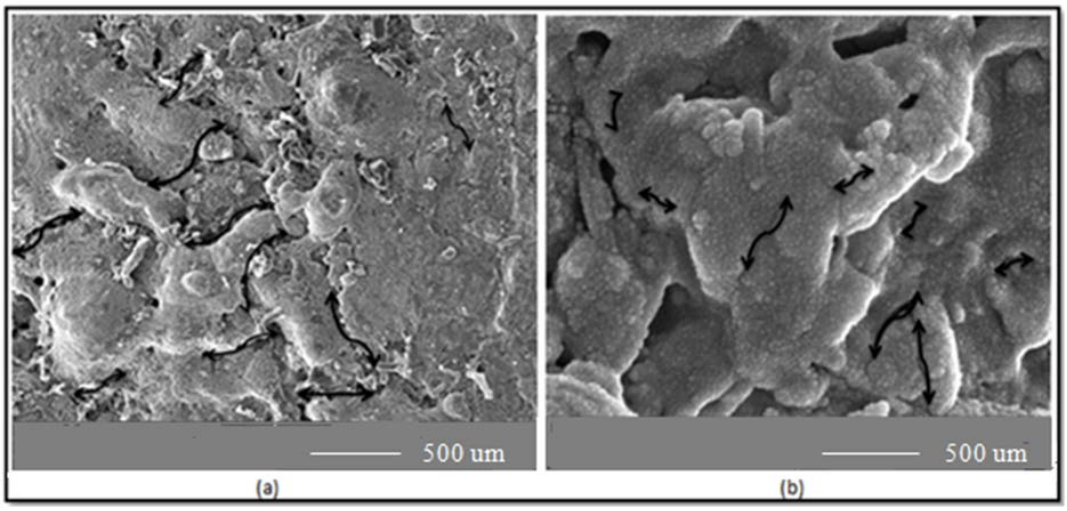

Figure 11. SEM Image of Surface Crack Density at voltage 50V and solution concentration 30% for a) A_1 alloy, b) A_2 alloy.

CONCLUSION

The following conclusions are made based on the results obtained:

1. Voltage machining (50,60,70, & 80) V and solution concentration (30 & 40) % have a high influence on the rate of material removal, wear rate of the tool, the thickness of the white layer, and surface roughness.
2. Addition silver and copper nanoparticles to base alloy improved the machining characteristics results.
3. Alloy A_2 has more MRR, TWR than A_1 alloy
4. Surface roughness, white layer thickness, and surface crack density for alloy A_2 lower than A_1 alloy.

REFERENCES

[1] Y.F. Zheng , B.B. Zhang , B.L. Wang, Y.B. Wang , L. Li , Q.B. Yang , L.S. Cui, "Introduction of antibacterial function into biomedical TiNi shape memory alloy by the addition of element Ag," *Acta*

Biomaterialia., vol. 7, PP. 2758–2767, 2011, DOI:10.1016/j.actbio.2011.02.010.

[2] B. Al-Zubaidy, N. S. Radhi, and Z. S. Al-Khafaji, 'Study the effect of thermal impact on the modelling of (titanium-titania) functionally graded materials by using finite element analysis', Int J Mech Eng Technol, no. 1, 2019.

[3] H. F. Li, K. J. Qiu, F. Y. Zhou, L. Li and Y. F. Zheng, " Design and development of novel antibacterial Ti-Ni-Cu shape memory alloys for biomedical application', *Scientific Reports* Vol.6, No.37475, 2016, DOI: 10.1038/srep37475.

[4] Lijo Paul and Somashekhar S Hiremath, "Improvement in Machining Rate with Mixed Electrolyte in ECDM Process," *Procedia Technology*, Vol. 25, PP:1250 – 1256, 2016, DOI: 10.1016/j.protcy.2016.08.218.

[5] Pfeifer R, Herzog D, Hustedt M, and Barcikowski S, " Pulsed Nd:YAG Laser Cutting of NiTi Shape Memory Alloys- influence of Process Parameters", *J Mater Process Technol*, Vol. 210, 2010, PP: 1918-1925.

[6] Kong MC, Srinivasu D, Axinte D, Voice W, McGourlay J, and Hon B," On Geometrical Accuracy and integrity of Surfaces in Multi-Mode Abrasive Water Jet Machining of NiTi Shape Memory Alloys", *CIRP Ann Manuf Technol* , Vol.62, 2013, PP:555-558.

[7] Mareike Frensemeier, Dominik Schirra, Martin Weinmann, Olivier Weber and Elmar Kroner, "Shape-Memory Topographies on Nickel–Titanium Alloys Trained by Embossing and Pulse Electrochemical Machining", *Advanced Engineering Materials*, Vol. 18, No. 8, 2016, DOI: 10.1002/adem.201600012.

[8] Ali Alidoosti, Ali Ghafari-Nazari, Fathollah Moztarzadeh, Newsha Jalali, Sina Moztarzadeh and Masoud Mozafari, "Electrical discharge machining characteristics of nickel–titanium shape memory alloy based on full factorial design", *Journal of Intelligent Material Systems and Structures*, 2013, DOI: 10.1177/1045389X13476147.

[9] Alana Witt Hansen, Luciane Taís Führ, Leonardo Marasca Antonini, Denis Jardim Villarinho, Claudia Eliana Bruno Marino and Celia de Fraga Malfatti, " The Electrochemical Behavior of the NiTi Alloy in Different Simulated Body Fluids", *Materials Research*, Vol. 18, No.1,PP: 184-190, 2015, DOI:10.1590/1516-1439.305614.

[10] Haydar Al-Ethari, Ali H., Noora M, "An Investigation on Chemical Machining of NiTi SMA Prepared by Powder Metallurgy", *2nd International Conference on Sustainable Engineering Techniques ,IOP Conf. Series: Materials Science and Engineering* 518, 032032, 2019, DOI: 10.1088/1757-899X/518/3/032032 .

[11] Robert Roth, Suat Coemert, Sarah Burkhardt, katia Silke Rodewald and Tim C. Lueth, "A Process towards Eliminating Cytotoxicity by Removal of Surface Contamination from Electrical Discharge Machined Nitinol", *BioManufacturing Conference*, Vol.89, PP: 45-51, 2020, DOI: 10.1016/j.procir.2020.05.117.

[12] A A Alhumdany, A K Abidali and H J Abdulredha, "Investigation of Wear Behaviour for NiTi Alloys with Yttrium and Tantalum Additions", *2nd International Conference on Engineering Sciences, IOP Conf. Series: Materials Science and Engineering*, Vol. 433, 2018, DOI:10.1088/1757-899X/433/1/012072.

[13] Margareta Coteaţa, Nicolae Pop, Hans-Peter Schulze, Laurenţiu Slatineanu and Oana Dodun," Investigation on hybrid electrochemical discharge drilling process using passivating electrolyte", *18th CIRP Conference on Electro Physical and Chemical Machining*, Vol. 42, PP:778 – 782, 2016, DOI: 10.1016/j.procir.2016.02.318.

[14] Lijo Paul and Somashekhar S. Hiremath, " Response Surface Modelling of Micro Holes in Electrochemical Discharge Machining Process", *International Conference On Design and Manufacturing, Procedia Engineering*, Vol. 64, PP: 1395–1404, 2013, DOI: 10.1016/j.proeng.2013.09.221.

[15] Biplab Kumar Roy and Amitava Mandal, " Surface integrity analysis of Nitinol-60 shape memory alloy in WEDM", *Materials and Manufacturing Processes*, ISSN: 1042-6914 (Print),1532-2475 (Online), 2019, DOI:10.1080/10426914.2019.1628256.

[16] Mallaiah Manjaiah and Rudolph Frans Laubscher, " Evaluation of wire electro discharge machining characteristics of Ti50Ni50-xCux shape memory alloys", *Journal of Materials Research*, 2016, DOI: 10.1557/jmr.2016.189.

[17] Ketaki Rajendra Kolhekar and Murali Sundaram, "A Study on the Effect of Electrolyte Concentration on Surface Integrity in Micro Electrochemical Discharge Machining", *3rd CIRP Conference on Surface Integrity*, Vol.45, PP:355–358, 2016, DOI: 10.1016/j.procir.2016.02.146.

[18] Saad K Shather, Shukry H. Aghdeab and Waqass S. Khudhier, " Enhancement the Thermal Effects Produce by EDM Using Hybrid Machining", *2nd International Conference on Sustainable Engineering Techniques, IOP Conf. Series: Materials Science and Engineering*, Vol. 518, IOP Publishing, 2019, DOI:10.1088/1757-899X/518/3/032016.

[19] Hargovind Soni, Narendranath S., and Ramesh M. R., "Effects of Wire Electro-Discharge Machining Process Parameterson the Machined Surface of Ti50Ni49Co1Shape Memory Alloy", *Silicon Journal*, 2018, DOI: 0.1007/s12633-017-9687-x.